

E-4.23

Separation System Synthesis for Fractional Crystallization from Solution Using a Network Flow Model

Luis A. Cisternas

Departamento de Ingeniería Química, Universidad de Antofagasta—Chile, Antofagasta, Chile

Ross E. Swaney*

Department of Chemical Engineering, University of Wisconsin, Madison, Wisconsin 53706

A method is presented to synthesize process flowsheets for separations of mixtures by fractional crystallization. Using equilibrium data for a candidate set of potential operating point temperatures, a network flow model is constructed to represent the set of potential separation flowsheet structures that can result. By employing specified approaches to multiple saturation point conditions, linear network constraints are obtained. Solution of the network flow model shows the optimal mass flow pattern between the candidate equilibrium states, and from this the corresponding process flowsheet is readily deduced. The method as presented is generally applicable to problems with two salts and one or more solvents, including systems forming one or more multiple salts or hydrates. Situations having multiple feeds and multicomponent products are also included. Several salt separation examples are given which demonstrate the method's application and show some of the types of coupled cycles that are obtained as solutions.

Introduction

The subject of separation system synthesis has received considerable attention in the literature due to the significant capital and operation costs associated with these processes. Much of the research has concerned the synthesis of distillation-based separation systems. To date, much less attention has been directed toward fractional crystallization from solution. Flowsheet synthesis procedures for these processes are not yet fully developed and form the subject of this paper.

The full subject of crystallization system design involves a broad range of issues pertaining to the operations employed, such as crystallization and dissolution kinetics, habit and size distribution, filtration and washing behavior, and solids handling. The focus of this paper, however, is on the overall process design and the determination of the optimal flowsheet structure. It is assumed that the practicality and economic costs of the operations to be employed either are known or will be determined as needed.

Fractional crystallization operations are deceptively simple methods of separating mixtures of salts that differ in solubility. The complete separation by crystallization of a ternary mixture (two salts and one solvent) is naturally limited by the presence of one or more points of multiple saturation (eutectics); two or more points of multiple saturation occur when one or more double salts are formed. Since two salts will crystallize out simultaneously when the multiple saturation point composition is reached, the maximum recovery of a single salt is limited by approach to that composition.

The usual method to overcome this limitation is fractional crystallization. Fractional crystallization employs a combination of heating, cooling, evaporation, dilution, and solid-liquid separation steps in a flow pattern which may include recycles.

The earliest published work on the flowsheet design of fractional crystallization processes is that of Fitch (1970), who developed systematized procedures by which ideal equilibrium processes can be designed from solubility data. That work identifies basic feasible cycles and suggests their use as building blocks in assembling systems to separate several components. However, the synthesis problem of identification and selection of alternatives is not addressed.

Ng (1991) presents a synthesis method for separation of solids based on selective crystallization and dissolution. The method can be applied to mixtures of solids that do not form double salts and have solubilities that are monotonically increasing or decreasing functions of temperature. Such systems cover only a subset of fractional crystallization problems. Also, the method is not applicable to the separation of salts from brine. Dye and Ng (1995b) investigate fractional crystallization of two- and three-solute mixtures that do not form hydrates or compounds. Specific one- and two-loop structures are examined. Berry and Ng (1996) address quaternary conjugate salt systems, proposing particular structures for three classes of solubility behavior. Berry et al. (1997) consider drowning-out (solventing-out) methods for two-solute systems, proposing seven structures suiting different equilibrium behavior and feed properties. Though addressing the more restricted problem of extractive crystallization, the works of Rajagopal et al. (1991) and Dye and Ng (1995a) present related ideas. Also, Berry and Ng (1997a,b) consider reactive crystallization and crystallization-distillation hybrids.

* To whom correspondence should be addressed. Telephone: (608) 262-3641. Fax: (608) 262-5434. E-mail: swaney@engr.wisc.edu.

Thomsen et al. (1995) investigate a particular two-crystallizer structure for one- and two-product processes and also present a method for generating phase diagrams.

Cisternas and Rudd (1993) present a systematic procedure for the identification of alternative process designs for ternary and multicomponent systems that form anhydrous and hydrated single salts, and anhydrous and hydrated double salts. However, their method does not include multiple feeds, multicomponent product streams, or stream-splitting possibilities. Also, their method does not apply if there is more than one double salt in the system.

In this paper, we present a method based on a network flow model for synthesis of fractional crystallization separation systems. The method can be applied to systems with two salts and one or more solvents, including multiple feeds, multicomponent products, and systems that form one or more multiple salts. With limitations it also has some applicability to systems with more than two solute products.

The spectrum of crystallization applications spans a broad range, from small-scale, high-purity requirement situations to large-scale bulk separations. The method presented here is most appropriate for large-scale processes. In these situations capital, maintenance, and often energy costs typically are significant and make the process economics sensitive to the magnitudes of the throughput rates of the operations and responsive to improvements in the flowsheet design.

The method presented here is based on an abstraction of the equipment operations into the phase equilibrium space. At this level, all of the crystallization, dissolution, evaporation, and dilution steps can be represented in terms of material flows between particular thermodynamic equilibrium states. Knowing the phases, compositions, and temperatures pertaining to each state, a network model can be constructed embodying all of the flow possibilities between the states. Solution of this representation as a network flow optimization problem yields the desired flowsheet.

Below, the network model is developed. Its use is then illustrated in a series of examples involving salt separations.

Model Development

Problem Statement. The fractional crystallization process design problem considered here can be stated as follows: Given a set of feeds containing a set of species (solutes and solvents) and a set of allowed candidate operating temperatures, synthesize a process flowsheet that will separate the feed streams into product streams of specified compositions at minimum total cost. The separations are to be performed by exploiting differences in solubilities. Operations may include dissolution, crystallization, solids separation, solvent removal, and mixing, conducted at any of the candidate operating temperatures.

Selection of Operating Temperatures. While the feed and product streams are defined by the separation task itself, the candidate operating temperatures will be selected based on two other factors. The first of these is the set of temperatures at which heating and cooling are available. The second is the temperature sensitivity of the phase diagram.

Heating and cooling availability will define which operating temperatures are possible, typically giving a

maximum and a minimum. Within this range, inspection of the phase equilibrium behavior will indicate whether or not operating points lying either at an extreme or within any particular intermediate range will provide or enable a potentially useful process feature. Simply changing the temperature often provides a compositional difference that can serve as the basis for a separation cycle. With more complicated equilibria, different temperatures can give rise to different precipitated species. The selection of operating temperature candidates is thus problem dependent, but sensible choices should be apparent. The method developed here has the capacity to handle a number of temperatures, so if the potential merit of a candidate temperature is not clear, it may be included anyway to cover the possibility.

Basic Assumptions. In constructing the model, two principal assumptions will be employed:

(1) A crystallizer or leaching is operated essentially at a point of multiple saturation. Operating at these points allows the maximum recovery of any solute. Since more than one solute may crystallize at a multiple saturation point, operation exactly at these points is not possible. Most often, however, practical operation is achieved very near to the actual multiple saturation point. For instance, in Perry et al. (1984), a 95–98% approach is reported as normally possible with inorganic salts.

(2) The combined investment and operating costs of industrial crystallizer systems are increasing functions of the evaporation, dilution, solids separation, and recycle flow rates. Principally, we assume that the process economics can be computed as a function of the individual flows within the process, given the operating conditions of each operation. At the simplest level, minimizing the total of the flow rates can be used as a surrogate for actual cost minimization. More elaborate cost functions with specific capital and operating cost terms may also be employed.

Model Formulation. Under the assumptions above, the mass flows comprising the process can be represented in terms of a network, with nodes corresponding to multiple saturation points, solute intermediate species, process feeds, and end products. Because more than one solute can be precipitated around a multiple saturation point, each of these points gives rise to multiple nodes in the network, one node for each possible solid that may be precipitated at that multiple saturation point. Solute intermediate nodes arise when the phase equilibrium gives solid phases that are not end products (e.g., double salts). Feed and product nodes in this formulation serve two roles. They provide for the input and output flows of the process feed and product streams. Beyond this, they also are used to provide for addition and removal of solvents to and from intermediate nodes. The flow rates for solvent feed and product nodes typically are left as variables, with implicit recycle of solvent.

Inputs to the intermediate and product nodes are mixed. Output streams from the feed and intermediate nodes have fixed compositions. For nodes engendered by multiple saturation points, these are given by the equilibrium compositions of the corresponding phases, or a specified approach thereto. Intermediate solute species nodes and feeds have defined compositions.

For the mathematical formulation we define the following sets and constants:

$$M = \{\text{multiple saturation point nodes}\} \quad (1)$$

$$S = \{\text{intermediate solute nodes}\} \quad (2)$$

$$I_F = \{\text{feed nodes}\} \quad (3)$$

$$I'_F = \{\text{feed nodes } i \in I_F \text{ with feed rates specified}\} \quad (4)$$

$$I = I_F \cup M \cup S \cup J_V \quad (5)$$

$$J_S = \{\text{solute product nodes}\} \quad (6)$$

$$J_V = \{\text{solvent product nodes}\} \quad (7)$$

$$J_P = J_S \cup J_V \quad (8)$$

$$J'_P = \{(j, k) = \text{product nodes } j \in J_P \text{ with flow rates of species } k \in K \text{ specified}\} \quad (9)$$

$$J = J_P \cup M \cup S \quad (10)$$

$$K = \{\text{species in the system (solutes and solvents)}\} \quad (11)$$

$$y_{ik}^{(i,j)} = \text{composition of phase } l \text{ from node } i, \text{ species } k \in K \quad (12)$$

$$l(i,j) = \text{phase of flow from node } i \text{ to node } j = \begin{cases} L \text{ (liquor)} & i \in M, j \in M \\ S \text{ (solute)} & i \in M, j \in (S \cup J_S); i \in S \\ V(j) \text{ (solvent)} & i \in M, j \in J_V \\ V(i) & i \in J_V \\ F \text{ (feed)} & i \in I_F \end{cases} \quad (13)$$

$$Y_{ij} = \{\text{species present in flow from node } i \text{ to node } j\} = \{k | y_{ik}^{(i,j)} \neq 0\} \quad (14)$$

$$\bar{Y}_j = \{\text{species not present at node } j\} = \{k | y_{jk}^L = 0, j \in M; y_{jk}^S = 0, j \in S; y_{jk}^V = 0, j \in J_V; P_{jk} = 0, (j, k) \in J'_P\} \quad (15)$$

$$X = \{\text{all possible internode species flows not disallowed by the } \bar{Y}_j\} = \{(i, j, k) | k \in Y_{ij}, Y_{ij} \cap \bar{Y}_j = \emptyset; i \in I, j \in J, k \in K\} \quad (16)$$

The determination of the set M and the compositions $y_{ik}^{(i,j)}$ of its member nodes is detailed in the Appendix.

The network flow optimization problem may be formulated in terms of either stream total flow rates or individual species flow rates. We will use the latter, with optimization variables x_{ijk} representing the flow rate of species k from node i to node j :

$$\min \sum_{(i,j,k) \in X} c_{ijk} x_{ijk} \quad (17)$$

$$\text{s.t. } \sum_{(i,m,k) \in X} x_{imk} = \sum_{(j,m,k) \in X} x_{jmk} \quad m \in (M \cup S), k \in K \quad (18)$$

$$\sum_{(i,j,k) \in X} x_{ijk} = F_{ik} \quad i \in I'_F, k \in K \quad (19)$$

$$\sum_{(i,j,k) \in X} x_{ijk} = P_{jk} \quad (j, k) \in J'_P \quad (20)$$

$$\left. \begin{aligned} x_{ijk} &= y_{ik}^{(i,j)} \sum_{k' \in K} x_{ij k'} \\ x_{ijk} &\geq 0 \end{aligned} \right\} (i, j, k) \in X \quad (21)$$

The network model constraints are comprised of species balances around the intermediate nodes (18), specifications of feed (19), and product rates (20) and the relations fixing the compositions of each source node (21). These all are linear, and together with flow nonnegativity they define a convex feasible region. We note that inequalities may be used in (19) and (20) when appropriate. In the case of a simple linear objective function as shown, a linear program results. The model may be solved using standard optimization packages, for example, GAMS (Brooke et al., 1997) or AMPL (Fourer et al., 1993).

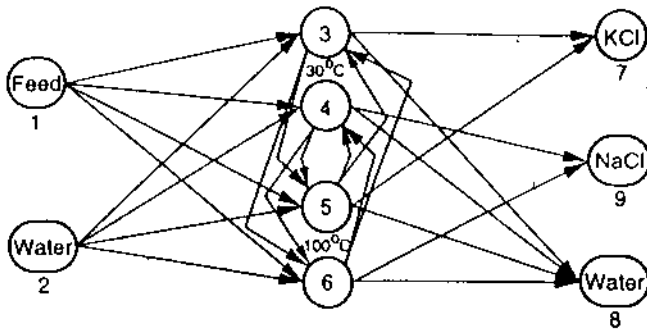
Solution of this model indicates the optimal flowsheet. The nonzero flows indicate the operating points employed in addition to the mass balance for the design. Equipment requirements to accomplish the implied crystallization, dilution, solids separation, evaporation, heating, cooling, and transport can be determined directly. Detailed design modelling and final optimization of the flows, operating conditions, and equipment parameters can then be completed using the flowsheet structure provided by the model.

Limitations of the Present Formulation. In the model as presented above in (17)–(22), the node compositions $y_{ik}^{(i,j)}$ are taken as constants, resulting in linear network constraints. When only one solid species is to remain or precipitate at any one intermediate node, appropriate compositions for the streams leaving the node can be determined a priori from a properly chosen approach distance to the multiple saturation condition. However, if two or more solid species are to remain or coprecipitate at a node, the relative proportions of the solids are not determined by the saturation conditions. Also, with more than two independent solutes present, the multiple saturation conditions can be approached over a range of solution compositions.

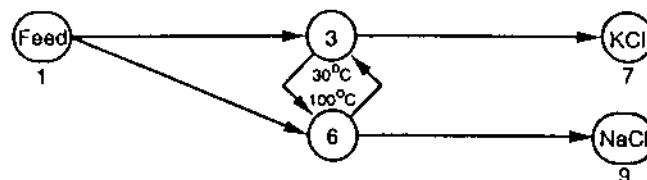
For two-solute separations, steps yielding more than one solid normally would not be needed, and the model is readily applied. With more than two solutes, the model can be applied to find processes that do not employ steps yielding multiple solids. This may be approached by gridding the ranges of solution compositions over the double saturation boundaries, introducing several nodes to sample over the ranges of interest. However, consideration of all important process options requires that nodes yielding multiple solids be included as well. The gridding approach could be extended to cover a range of mixed solids compositions, with nodes sampling over the additional composition combinations. The model has the capacity to accommodate a large number of such nodes, even though practical limitations will eventually be reached with a large number of solutes. This approach for multiple solutes remains to be more fully examined.

Table 1. Solubility Data for the System KCl–NaCl–H₂O saturated solution, wt %

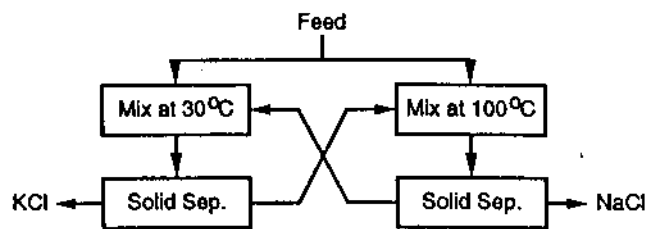
temp. °C	KCl	NaCl	H ₂ O	NH ₃	solid phases
30	11.70	20.25	68.05	0.0	KCl, NaCl
100	22.20	15.90	61.9	0.0	KCl, NaCl
25	1.0	16.2	42.8	40.0	KCl, NaCl



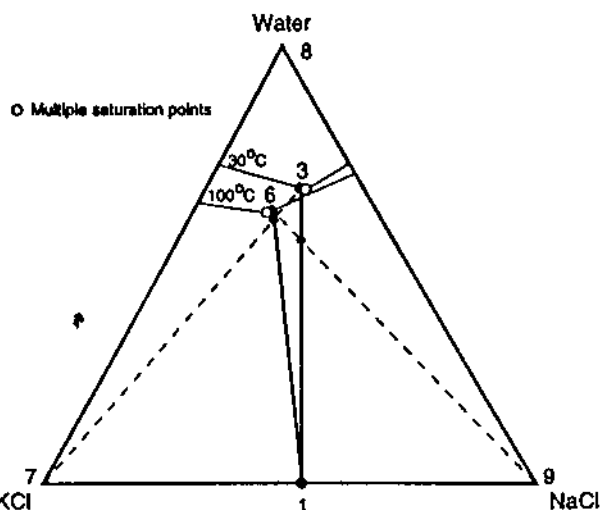
(a)



(b)



(c)



(d)

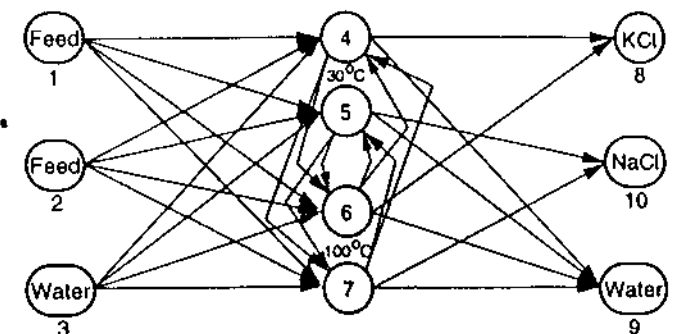
Figure 1. Example 1.1: KCl from sylvinitic. (a) Network structure. (b) Solution flows. (c) Corresponding flowsheet. (d) Paths on the phase diagram.

Examples

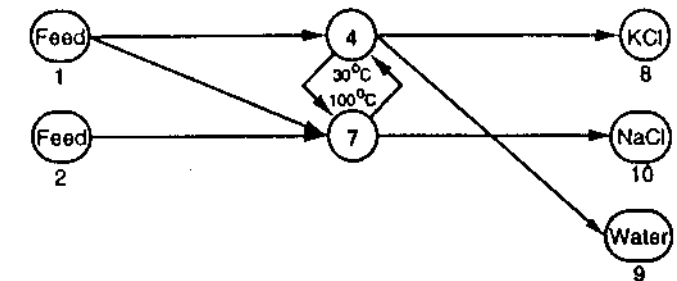
In the examples below, zero approaches to multiple saturation compositions were employed for simplicity,

Table 2. Example 1.1: Flow Rates for the Optimal Network in Figure 1b

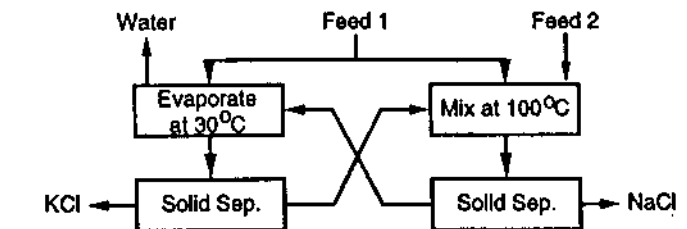
	flow rate, f_{ij}				$\sum c_{ijk}$	
	f_{13}	f_{16}	f_{37}	f_{69}	f_{37}	f_{69}
KCl	7.912	39.788	36.639	47.700	76.427	
NaCl	8.675	43.625	63.443		54.738	52.300
water			213.099		213.099	



(a)



(b)



(c)

Figure 2. Example 1.2: KCl from sylvinitic with two feeds. (a) Network structure. (b) Solution flows. (c) Corresponding flowsheet.

and a simple minimum-flow objective function was used (all $c_{ijk} = 1$).

Example 1: Production of KCl from Sylvinitic. Consider the production of potassium chloride from 100 units of sylvinitic (47.7% KCl, 52.3% NaCl). The separation of sylvinitic using dilution and crystallization has been studied by Rajagopal et al. (1988) and by Cisternas and Rudd (1993). Both papers find that there are two alternative structures for the separation and that the optimal structure is that of leaching → NaCl filtration → crystallization → KCl filtration.

Here, three cases are studied. In example 1.1, we seek the optimal structure using water as solvent. Example 1.2 considers the case where there are two feeds with different compositions. In example 1.3, the possibility of using water and ammonia as solvents is studied.

Data on phase equilibrium for the system KCl–NaCl–H₂O from Linke and Seidell (1965) are given in

Table 3. Example 1.2: Flow Rates for the Optimal Network in Figure 2b

	flow rate, $f_{ij} = \sum_k v_{k,ij}$							
	f_{14}	f_{17}	f_{17}	f_{17}	f_{18}	f_{19}	f_{24}	$f_{7,10}$
KCl	10.784	36.916	25.000	55.364	72.700		117.279	
NaCl	11.824	40.476	70.000	95.822			83.997	122.300
water			5.000	322.008		5.000	327.008	

Table 4. Example 1.3: Flow Rates for the Optimal Network in Figure 3b

	flow rate, $f_{ij} = \sum_k v_{k,ij}$							
	f_{17}	f_{18}	f_{18}	f_{18}	$f_{7,12}$	$f_{7,13}$	f_{87}	$f_{8,10}$
KCl	35.841	11.859		38.338			2.498	47.700
NaCl	39.297	13.003		27.459	52.300		40.461	
water				106.898			106.898	
ammonia		99.905			99.905	99.905		

Table 5. Points of Multiple Saturation for the System $\text{Na}_2\text{CO}_3\text{-Na}_2\text{SO}_4\text{-H}_2\text{O}$

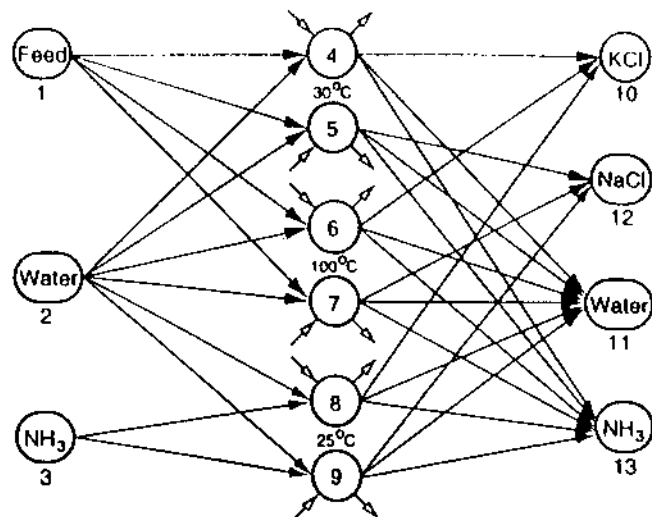
key	temp, °C	saturated solution, wt %		solid phases
		Na_2CO_3	Na_2SO_4	
C	20	14.95	11.2	$\text{Na}_2\text{CO}_3 \cdot 10\text{H}_2\text{O}$, $\text{Na}_2\text{SO}_4 \cdot 10\text{H}_2\text{O}$
H1	50	11.4	22.2	$\text{Na}_2\text{CO}_3 \cdot 2\text{Na}_2\text{SO}_4$, Na_2SO_4
H2	50	29.7	5.5	$\text{Na}_2\text{CO}_3 \cdot \text{H}_2\text{O}$, $\text{Na}_2\text{CO}_3 \cdot 2\text{Na}_2\text{SO}_4$

Table 1. Two temperatures are considered as multiple saturation points, 30 and 100 °C. Also included in Table 1 are data for the KCl-NaCl-H₂O-NH₃ system at 25 °C given by Gaska et al. (1965).

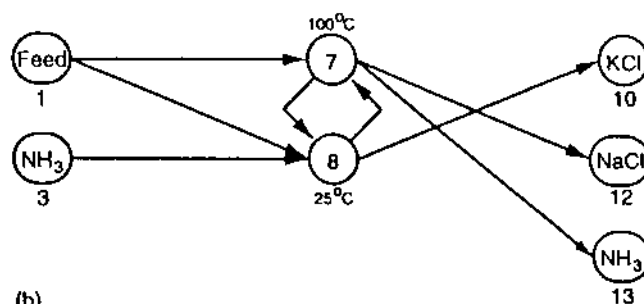
Example 1.1. Figure 1 shows the structure of the full network, the solution to the network flow problem, and the flowsheet structure corresponding to the solution. The network structure in Figure 1a employs nine nodes. Node 1 is the sylvinite feed node. Nodes 3 and 4 correspond to the multiple saturation point at the cold temperature (30 °C). Node 3 allows the separation of KCl, whereas node 4 allows the separation of NaCl. In the same way, nodes 5 and 6 correspond to the multiple saturation point at the hot temperature (100 °C), allowing the separation of KCl and NaCl, respectively. Nodes 7-9 are product nodes, with nodes 7 and 9 being the solute products (pure salts). All allowed flows between the nodes are shown in the figure. Flow is allowed from the feed node 1 to nodes 3-6. Water can be added from node 2 (dilution), or removed to node 8 (evaporation), to or from the multiple saturation nodes 3-6.

Figure 1b shows the solution to the network flow optimization problem. The corresponding flow rates are given in Table 2, and the corresponding flowsheet is shown in Figure 1c. Figure 1d shows the process paths on the phase diagram. The solution found is not the same as that found by Rajagopal et al. (1988) and Cisternas and Rudd (1993), where all the sylvinite was fed to the hot point of multiple saturation and where both dilution and evaporation were needed to achieve the separation. The optimal solution divides the feed into two parts, with 16.6% fed to the cold point of multiple saturation and 83.4% fed to the hot point of multiple saturation. Neither evaporation nor dilution is needed.

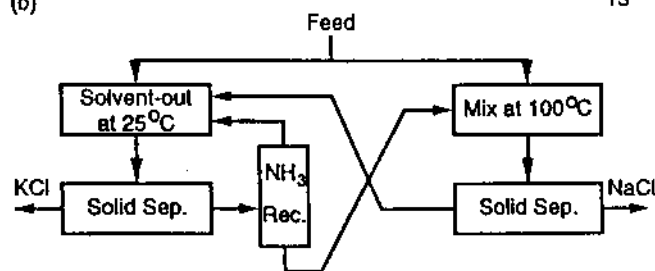
Example 1.2. Sometimes two different types of sylvinite are available. This example analyzes the flowsheet structure for such a situation. Potassium chloride product is to be produced from the combination of 100 units of feed 1, a sylvinite of composition 47.7%



(a)



(b)



(c)

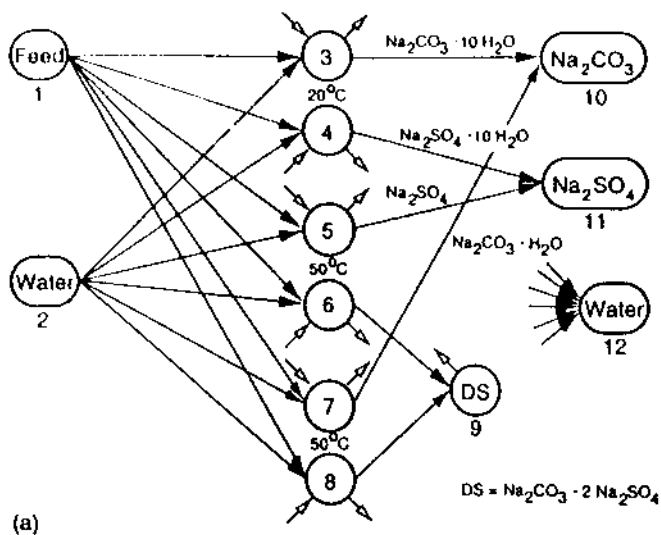
Figure 3. Example 1.3: Sylvinitic system with ammonia. (a) Network structure. (b) Solution flows. (c) Corresponding flowsheet.

KCl and 52.3% NaCl by weight, and 100 units of feed 2, a sylvinite with composition 25% KCl, 70% NaCl, and 5% H₂O.

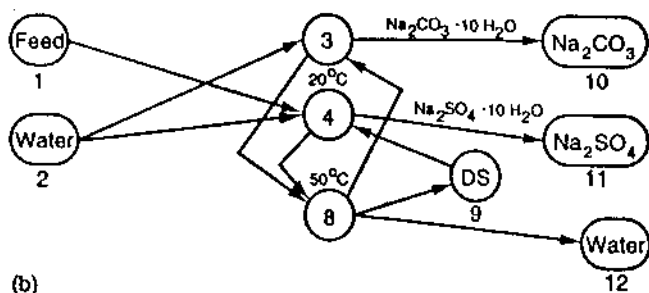
Figure 2a shows the network structure for this case. Node 2 has been added to the network of the previous example to represent feed 2, giving a total of 10 nodes in the network.

Figure 2b shows the nonzero flows appearing in the solution to the network flow optimization. The corresponding flow rates are given in Table 3, and the corresponding flowsheet is shown in Figure 2c. The optimal solution divides feed 1 into two parts, so that 22.61% is fed to the cold multiple saturation point and 77.39% is fed to the hot multiple saturation point. Feed 2 is fed in its entirety to the hot multiple saturation point. Evaporation is required at the cold multiple saturation point, but dilution of the feed is not necessary.

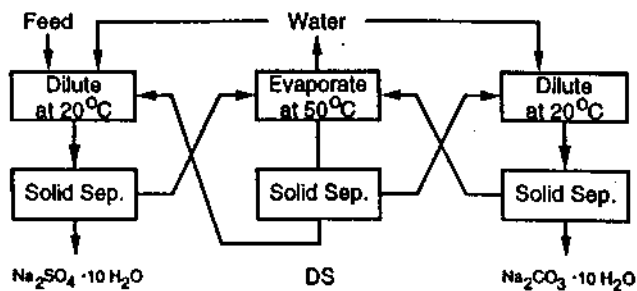
Example 1.3. Several studies have considered the use of ammonia to solvent-out potassium chloride (Gaska et al., 1965). This example analyzes the flowsheet structure when ammonia is also allowed in the



(a)



(b)



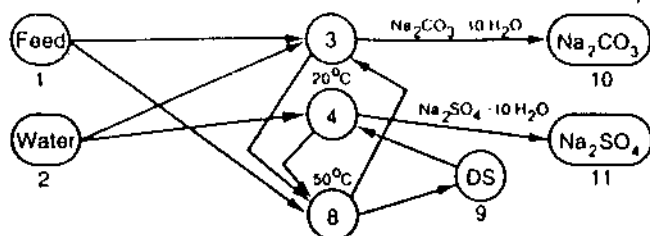
(c)

Figure 4. Example 2: Na_2CO_3 - Na_2SO_4 - H_2O separation. Example 2.1: (a) Network structure. (b) Solution flows. (c) Corresponding flowsheet.

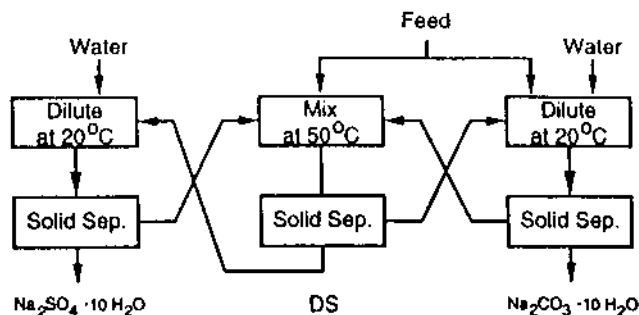
system. The equilibrium data for the KCl - NaCl - H_2O - NH_3 system at 25 °C is included in Table 1.

The network structure shown in Figure 3a employs 13 nodes, obtained by treating ammonia as an additional "solvent" and adding nodes 3, 8, 9, and 13 to the original network of Figure 1a. Nodes 8 and 9 represent the multiple saturation point with ammonia, with node 8 for the separation of KCl and node 9 for the separation of NaCl . Nodes 3 and 13 represent dilution with or removal of ammonia. In the figure, the open arrows represent the numerous interconnecting paths that have been omitted for clarity. The model includes the full set of paths indicated by the set X in (16).

Figure 3b shows the nonzero network flows in the solution. The flow rates in the network are given in Table 4, and the corresponding flowsheet is shown in Figure 3c. The optimal solution divides the feed into two parts, so that 75.14% is fed to the hot multiple saturation point and 24.86% is fed to the multiple



(a)



(b)

Figure 5. Example 2.2: (a) Solution flows. (b) Corresponding flowsheet.

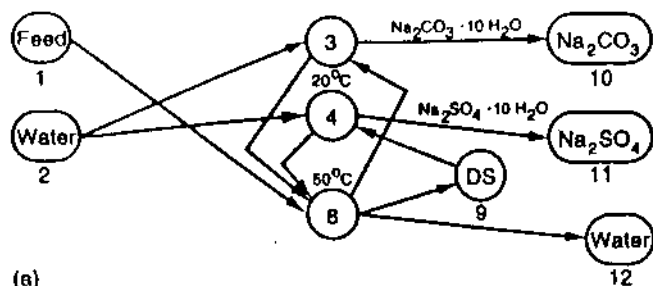
saturation point with ammonia. The cold multiple saturation point is not used as an operating point.

Note that, in the network representation in Figure 3b, ammonia solvent leaves node 7 in a separate pure stream. This implies a method of separating ammonia from the other solvent as well as the solutes. In this example the receiving node 7 is ammonia-free, implying separation of the ammonia from the feed liquid coming from node 8 before the liquid-solid-vapor equilibrium of the node 7 multiple saturation point is achieved. An ammonia recovery unit is needed as shown in Figure 3c.

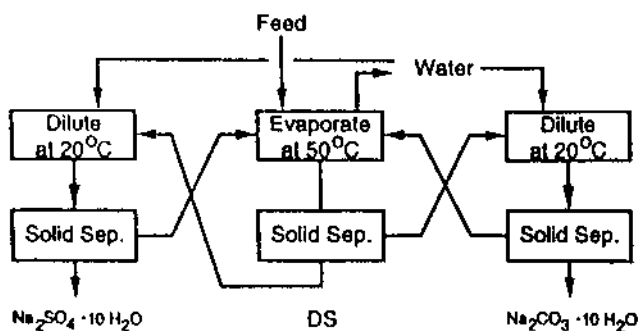
Example 2: Separation of Sodium Carbonate and Sodium Sulfate. Consider the separation of Na_2CO_3 and Na_2SO_4 from mixtures of those salts. Phase diagram data are available in Linke and Seidell (1965). This system presents both a temperature region where no double salts are formed and a temperature region where there is double salt formation. Table 5 shows the equilibrium compositions at two temperatures, 20 and 50 °C.

Several examples will be studied. First, in example 2.1, the feed will be the double salt burkeite, $\text{Na}_2\text{CO}_3 \cdot 2\text{Na}_2\text{SO}_4$. This example has been studied by Cisternas and Rudd (1993). In example 2.2, the feed is composed of 80% Na_2CO_3 and 20% Na_2SO_4 by weight. In example 2.3, the feed is an aqueous solution of 30% Na_2CO_3 and 20% Na_2SO_4 .

Figure 4a shows the network for these examples. For the three cases, the network structure remains the same but the composition of the feed (node 1) differs. There are 12 nodes total, with nodes 3-8 corresponding to multiple saturation points. Node 9 allows the processing of the double salt. Figures 4b, 5a, and 6a show the solutions for the three cases. The solution to example 2.1 includes two dilution steps and one evaporation step. The cold multiple saturation point is used twice, once for precipitation of sodium sulfate and once for precipitation of sodium carbonate. Only one of the two hot multiple saturation points is used (node 8), at which the double salt burkeite is precipitated. The solution to example 2.2 is similar to the solution of



(a)



(b)

Figure 6. Example 2.3: (a) Solution flows. (b) Corresponding flowsheet.

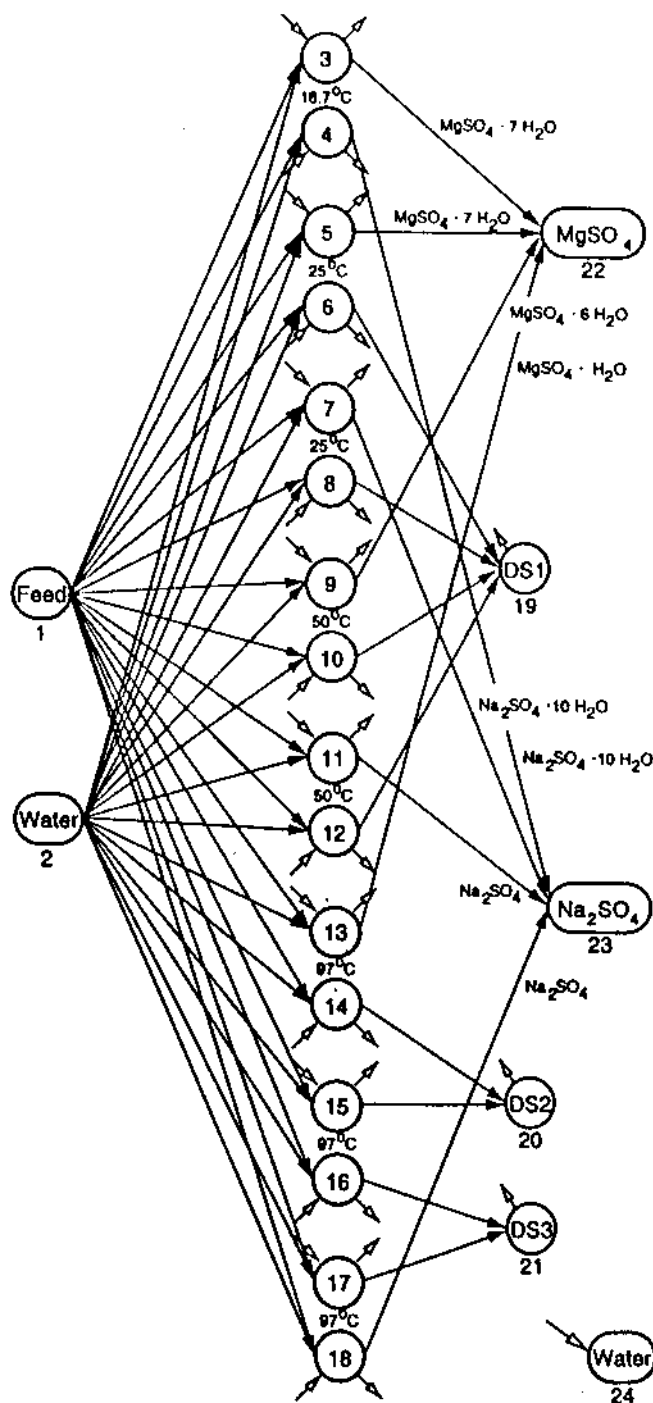
 Table 6. Points of Multiple Saturation for the System $\text{MgSO}_4\text{-Na}_2\text{SO}_4\text{-H}_2\text{O}$

key	temp. °C	saturated solution, wt %		solid phases
		MgSO_4	Na_2SO_4	
C1	18.7	20.57	11.80	$\text{MgSO}_4 \cdot 7\text{H}_2\text{O}$, $\text{Na}_2\text{SO}_4 \cdot 10\text{H}_2\text{O}$
C2	25	21.15	13.0	$\text{MgSO}_4 \cdot 7\text{H}_2\text{O}$, $\text{MgSO}_4 \cdot \text{Na}_2\text{SO}_4 \cdot 4\text{H}_2\text{O}$
C3	25	16.6	17.8	$\text{Na}_2\text{SO}_4 \cdot 10\text{H}_2\text{O}$, $\text{MgSO}_4 \cdot \text{Na}_2\text{SO}_4 \cdot 4\text{H}_2\text{O}$
H1	50	31.32	4.74	$\text{MgSO}_4 \cdot 6\text{H}_2\text{O}$, $\text{MgSO}_4 \cdot \text{Na}_2\text{SO}_4 \cdot 4\text{H}_2\text{O}$
H2	50	11.98	23.25	$\text{MgSO}_4 \cdot \text{Na}_2\text{SO}_4 \cdot 4\text{H}_2\text{O}$, Na_2SO_4
H3	97	32.20	5.55	$\text{MgSO}_4 \cdot \text{H}_2\text{O}$, $\text{MgSO}_4 \cdot \text{Na}_2\text{SO}_4$
H4	97	14.40	19.15	$\text{MgSO}_4 \cdot \text{Na}_2\text{SO}_4$, MgSO_4
H5	97	5.88	26.90	$\text{MgSO}_4 \cdot 3\text{Na}_2\text{SO}_4$, Na_2SO_4

example 2.1, but now the feed is divided into two parts, which allows elimination of the evaporation step. In example 2.3 where the feed is an aqueous solution, the feed is added to the hot multiple saturation point.

Example 3: Separation of Magnesium Sulfate and Sodium Sulfate from Astrakanite. Consider the separation of magnesium sulfate and sodium sulfate from the double salt astrakanite, $\text{MgSO}_4 \cdot \text{Na}_2\text{SO}_4 \cdot 4\text{H}_2\text{O}$. Data for the phase diagram is available in Linke and Seidell (1965). This system presents both temperature regions where double salts will form and regions where they will not form, as in the previous example. But here there may be several double salts depending on the temperature and composition. Table 6 shows the equilibrium compositions at several temperatures. At 97 °C, the system has two double salts, and therefore three double saturation points.

Figure 7 shows the network for this problem. There are 24 nodes, with nodes 3–18 being multiple saturation nodes. Nodes 19–21 allow processing of the double salts. Figure 8a shows the network flow optimal solution, and the flow rates are given in Table 7. This example demonstrates the ability of the network flow method to choose from among several alternate points of multiple saturation and alternative intermediate solutes.



DS1 = $\text{MgSO}_4 \cdot \text{Na}_2\text{SO}_4 \cdot 4\text{H}_2\text{O}$
 DS2 = $\text{MgSO}_4 \cdot \text{Na}_2\text{SO}_4$
 DS3 = $\text{MgSO}_4 \cdot 3\text{Na}_2\text{SO}_4$

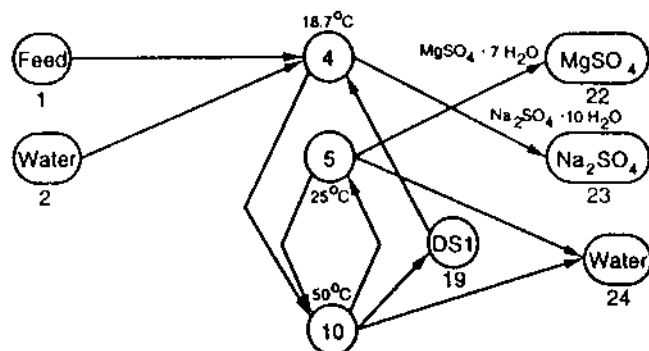
 Figure 7. Example 3: $\text{MgSO}_4\text{-Na}_2\text{SO}_4\text{-H}_2\text{O}$ separation with double salts. Network structure.

Conclusions

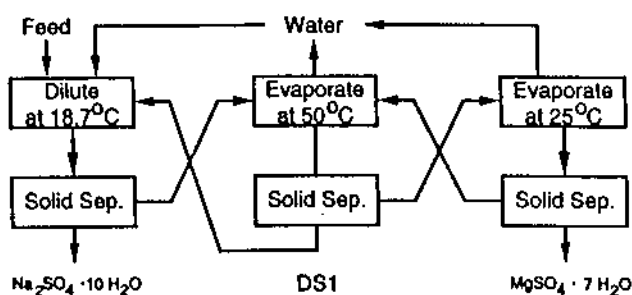
The network flow model presented here offers a straightforward and useful method for determining the desired process flowsheet for fractional crystallization processes. For a prespecified set of candidate operating temperatures and multiple saturation points, the model contains within it the set of all feasible flow patterns involving crystallization, dilution, and mixing operations at those conditions. The solution to the network flow optimization problem indicates the underlying mass flows of the desired flowsheet.

Table 7. Example 3: Flow Rates for the Optimal Network in Figure 8a

	flow rate, f_{ij} $\sum_{i,j} c_{ij}$									
	f_{11}	f_{14}	$f_{4,10}$	$f_{4,23}$	$f_{5,10}$	$f_{5,22}$	$f_{5,23}$	$f_{10,24}$	$f_{10,19}$	$f_{19,24}$
MgSO ₄	36.00		70.074		11.759	36.000		47.759	34.074	34.074
Na ₂ SO ₄	42.470		40.198	42.470	7.228		7.228	40.198	40.198	40.198
water	21.530	242.316	230.390	53.834	36.612	37.680	23.209	97.501	20.378	149.123



(a)



(b)

Figure 8. Example 3: (a) Solution flows. (b) Corresponding flowsheet.

The primary advantage of the approach lies in its ability to consider general process flow patterns. It is not necessary to adopt the restricting viewpoint that the flowsheet be comprised of a sequence of separation steps, or a simple cycle. Indeed, as the examples presented here show, the best flow pattern may often employ multiple coupled cycles. General flow patterns not only can lead to lower total throughput costs but sometimes can allow some evaporation or dilution steps to be eliminated.

A further advantage lies in the ability of the method to readily handle systems forming one or several double salts. In such problems it is not immediately apparent which solute species should be employed as intermediates in the separation; the network model determines this automatically. Problems with multiple feeds are also readily treated.

Since the model constraints are linear and since only a small number of nodes are required, the network optimization problem can be easily solved with standard algorithms. Useful results may be obtained from the model using linear costs, as demonstrated by the examples presented. With mixed-integer linear, continuous convex nonlinear, or mixed-integer convex nonlinear costs, available standard algorithms again should be quite adequate. Given the small sizes involved, it also may be practical to solve problems having general nonconvex costs functions using recently developed global optimization algorithms.

The model as introduced here is basic and does not include features such as wash solvent flows and heat integration. However, the network flow model has a

flexible structure and is amenable to such further developments.

Acknowledgment

This work was supported in part by the Fundación Andes-Chile (L.A.C.). Additional support was provided by University of Wisconsin for R.E.S. as a Vilas Associate.

Appendix

The network model includes a set of nodes M which are engendered by multiple saturation points. The following describes how these nodes are determined, given a specified set \hat{M} of multiple saturation points.

Let the set of all solutes present be denoted as $Q = S \cup J_s$. At a given multiple saturation point $m \in \hat{M}$, the solutes may be partitioned into those that are saturated with respect to their solid phase, $Q_s(m)$, and those that are unsaturated, $Q_u(m)$, with $Q_s \cup Q_u = Q$. The identity of the multiple saturation point is given by the membership of set $Q_s(m)$ and the saturation temperature T_m .

The liquid composition y_m^L of a multiple saturation point m is determined jointly by the saturation conditions at T_m for the solutes $j \in Q_s$. Let the phase equilibrium saturation boundary for each solute j be denoted by the following implicit equation for the liquid composition y^L :

$$f^s_j(y^L, T_m) = 0 \quad (23)$$

Then the composition of the multiple saturation point is given by the intersection of the solute saturation boundaries

$$f^s_j(y_m^L, T_m) = 0, \quad j \in Q_s \quad (24)$$

A given multiple saturation point $m \in \hat{M}$ with composition y_m^L gives rise to more than one network node. Consider the case where the dissolution and crystallization steps do not yield mixed solute solids. Then there can be as many nodes per multiple saturation point m as there are saturated solutes, i.e., $\#Q_s$. The composition of each of these nodes i is determined by the saturation condition for the one solute $q(i)$ coexisting as solid, combined with specified subsaturation requirements on the remaining solutes:

$$f^s_{q(i)}(y_{ij}^L, T_m) = 0 \quad (25)$$

$$y_{ij}^L = \hat{y}_{mj}^L - \epsilon_{ij}, \quad j \in (Q_s(m) - \{q(i)\}) \quad (26)$$

Here $\epsilon_{ij} \geq 0$ is the allowable approach to the saturation composition for solute species j . In this manner, each node i is identified with a liquid composition y_i^L and a solid species $q(i)$. The union of all such nodes i generated for all of the multiple saturation points $m \in \hat{M}$ gives the set M .

Literature Cited

- Berry, D. A.; Ng, K. M. Separation of Quaternary Conjugate Salt Systems by Fractional Crystallization. *AIChE J.* **1996**, *42*, 2162.
- Berry, D. A.; Ng, K. M. Synthesis of Reactive Crystallization Processes. *AIChE J.* **1997a**, *43*, 1737.
- Berry, D. A.; Ng, K. M. Synthesis of Crystallization-Distillation Hybrid Separation Processes. *AIChE J.* **1997b**, *43*, 1751.
- Berry, D. A.; Dye, S. R.; Ng, K. M. Synthesis of Drowning-Out Crystallization-Based Separations. *AIChE J.* **1997**, *43*, 91.
- Brooke, A.; Kendrick, D.; Meeraus, A.; Raman, R. *GAMS Language Guide*, GAMS Development Corp., 1997.
- Cisternas, L. A.; Rudd, D. F. Process Design for Fractional Crystallization from Solution. *Ind. Eng. Chem. Res.* **1993**, *32*, 1993.
- Dye, S. R.; Ng, K. M. Bypassing Eutectics with Extractive Crystallization: Design Alternatives and Tradeoffs. *AIChE J.* **1995a**, *41*, 1456.
- Dye, S. R.; Ng, K. M. Fractional Crystallization: Design Alternatives and Tradeoffs. *AIChE J.* **1995b**, *41*, 2427.
- Fitch, B. How to Design Fractional Crystallization Processes. *Ind. Eng. Chem.* **1970**, *62*, 6.
- Fourer, R.; Gay, D. M.; Kernighan, B. W. *AMPL: A Modeling Language for Mathematical Programming*; Scientific Press: San Francisco, CA, 1993.
- Gaska, R. A.; Goodenough, R. D.; Stuart, A. Ammonia as a Solvent. *Chem. Eng. Prog.* **1965**, *61*, 139.
- Lanke, W. F.; Seidell, A. *Solubilities of Inorganic and Metal Organic Compounds*; American Chemical Society: Washington, DC, 1965.
- Ng, K. M. Systematic Separation of a Multicomponent Mixture of Solids Based on Selective Crystallization and Dissolution. *Sep. Technol.* **1991**, *1*, 108.
- Perry, R. H.; Green, D. W.; Maloney, J. O. *Perry's Chemical Engineer's Handbook*, 6th ed.; McGraw-Hill: New York, 1984.
- Rajagopal, S.; Ng, K. M.; Douglas, J. M. Design of Solids Processes: Production of Potash. *Ind. Eng. Chem. Res.* **1988**, *27*, 2071.
- Rajagopal, S.; Ng, K. M.; Douglas, J. M. Design and Economic Trade-Offs of Extractive Crystallization Processes. *AIChE J.* **1991**, *37*, 437.
- Thomsen, K.; Gani, R.; Rasmussen, P. Synthesis and Analysis of Processes with Electrolyte Mixtures. *Comput. Chem. Eng.* **1995**, *19*, S27.

Received for review May 12, 1997

Revised manuscript received March 30, 1998

Accepted April 1, 1998

IE970335Y

